ACS OMEGA

http://pubs.acs.org/journal/acsodf

Article

Mechanistic Study of Micro-bubble Fluid Infiltration through the Fractured Medium

Sina Baseli Zadeh, Ehsan Khamehchi,* Saeed Saber-Samandari, and Ali Alizadeh

Cite This: ACS Omega 2022, 7, 26246−26255

Read Online

ACCESS | Metrics & More | Article Recommendations

ABSTRACT: Drilling in depleted reservoirs has many challenges due to the overbalance pressure. Another trouble associated with overbalance drilling is differential sticking and formation damage. Low-density drilling fluid is an advanced method for drilling these depleted reservoirs and pay zones with different pressures to balance the formation pore pressure and hydrostatic drilling fluid pressure. This study investigated the infiltration of a micro-bubble fluid as an underbalanced drilling method in fractured reservoirs. A novel method has been presented for drilling permeable formations and depleted reservoirs, leading to an impressive reduction in costs, high-tech facilities, and drilling mud invasion. It also reduces mud loss, formation damages, and skin effects during the drilling operation. This paper studied micro-bubble fluid infiltration in a single fracture, and a synthetic metal plug investigated the bridging phenomenon through the fractured medium. Moreover, the effects of fracture size, bubble size, and a pressure differential of fracture ends have been thoroughly analyzed, considering the polymer and surfactant concentrations at reservoir conditions, including the temperature and overburden pressure. In this study, nine experimental tests were designed using the design of experiment, Taguchi method. The results indicated that higher micro-bubble fluid mixing speed values make smaller bubbles with lower blocking ability in fracture (decrease the chance of blocking more than two times). On the other hand, a smaller fracture width increases the probability of bubble bridges in the fracture but is not as crucial as bubble size. As a result, drilling fluid infiltration in fractures and formation damages decreases in the condition of overbalanced drilling pressure differences of about 200 psi.

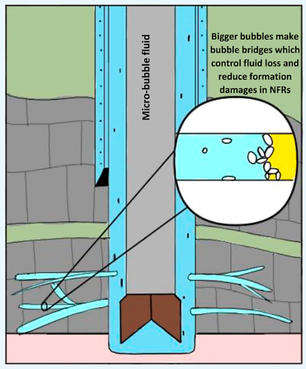

1. INTRODUCTION

One of the most important challenges in petroleum engineering is drilling reservoir formation. For example, drilling in overbalanced conditions can cause formation damage and fluid loss due to drilling fluid invasion into the production layer. In order to control the fluid loss and formation damage, various types of loss control materials (LCMs) can be used in mud, but these materials cause an adverse skin effects.[1] The low-density drilling fluid method can be used, provided that the costs and complicated equipment are limited, and He[2] summarized the field applications and laboratory study of aphron-based drilling fluid for past and future studies.

In order to lower the density of mud, air injection in the fluid and producing bubbles in the drilling mud has been previously investigated.[3] Ivan et al.[4] described the development and application of the micro-bubble drilling fluid experimentally and generated appropriate formulations, the operational procedures, and field applications. These bubbles are not stable, may disappear at higher pressures or temperatures, and have short longevity and weak pore-blocking ability.[5] Micro-bubble drilling fluid has been introduced for drilling permeable zones. Adding some polymers and surfactants can help produce micro-bubbles in the drilling fluid with non-coalescing and low-density properties using simple techniques. This drilling fluid can control mud loss through the permeable zone, causing pore and fracture blockage. This method reduces fluid invasion and also well skin because the first backwash moves the residual drilling fluid and bubbles into the well again.[6]

A micro-bubble fluid is a stable and non-coalescing fluid with 10−100 μm diameter, which Sebba introduced in 1987.[7] Some researchers such as Ramirez et al.[8] presented field results obtained by assessing the micro-bubble aphron system as the drilling mud in real wells. In another study, Brookey et al[1c] studied micro-bubble fluid as an underbalanced drilling fluid, which was proved to be a solution for controlling mud loss for drilling depleted reservoirs. At the beginning of the 21st century, Growcock et al.[3a] studied micro-bubble drilling fluid loss in porous media and showed lower formation damage compared to common LCMs. These physical properties of the fluid and the effects of the surfactant and polymer concentration were studied in micro models by ref 9. Two years later, Spinell et al.[10] proved the ability of micro-bubble drilling fluid to reduce mud filtration

Received: March 30, 2022
Accepted: June 29, 2022
Published: July 22, 2022

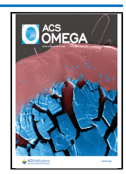

in the reservoir formation and demonstrated the impacts of surfactant on drilling fluid surface tension. In the following years, several studies were performed on micro-bubble fluid rheology and filtration criteria in various polymer and surfactant concentrations. Bubble size distribution, fluid stability, rheological models, bridging ability, impacts of water-based or oil-based muds, flow rate, fluid composition, permeability, and rock wettability were studied.[11] Zheng et al.[12] addressed rheological issues and optimized the rheological parameter of micro-bubble drilling fluids by multiple regression experimental design.

Recent publications modeled a single bubble in deviated gas wells' temperature and pressure.[13] The stability of water-based bubbles and flow in porous media were studied by ref 14. Later, they worked on a model for predicting size distribution and liquid drainage from micro-bubble fluids using population balance equations.[15] Keshavarzi et al.[16] used different surfactants and compared their stabilities and also the impacts of mixing speed and time on bubble size and stability.

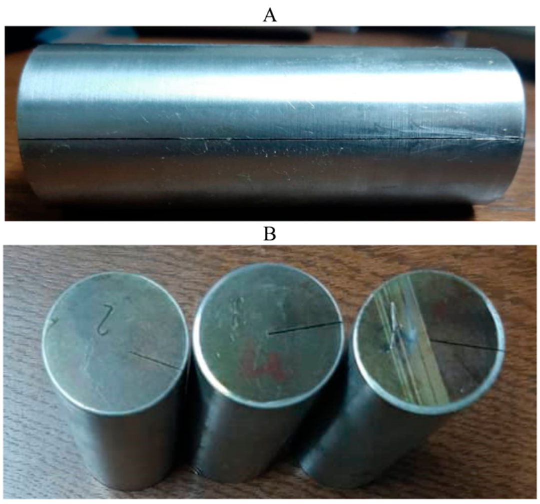

Figure 1. Top view of the core plug (A)—metal core plugs (B).

Table 1. Characteristics of Previously Studied Stable Micro-bubble Fluid Composition

NaOH (caustic soda)	SDBS	XG (gr/L)
about 1 gr/L	0.9 gr/L	3

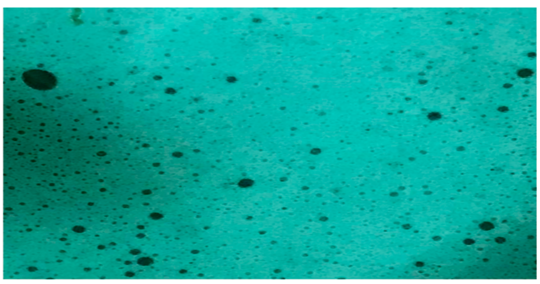

Figure 2. Micro-bubble fluid illustration.

There are several studies about micro-bubble drilling fluid penetration in porous media and fractures. The other researchers presented various aspects of these phenomena in their studies such as bubble size distribution, drainage rate, temperature, and pressure effects on micro-bubble fluid infiltration and bubble behavior modeling by mass-transfer concepts.[13−15] In addition, micro-bubbles size and rheological and filtration characteristics of colloidal gas aphron drilling fluids for a high-temperature well was investigated by ref 17. Le et al.[18] employed a new class of design of experiment (DOE) with definitive screening design to study the effect of five quantitative parameter of salinity, sodium dodecyl sulfate surfactant concentration, xanthan gum (XG) polymer concentration, mixing rate, and mixing time. They showed that the stability depends on the XG polymer and the sodium dodecyl sulfate surfactant concentration and stirring rate, but it decreases with increasing salinity. Zhu et al.[19] developed a new XG derivative synthesized by grafting acrylic acid, acrylamide, 2-acrylamido-2-methylpropane sulfonic acid onto XG and CGA drilling fluids with a temperature resistance of 180° generated by using XG.

In the latest experimental research studies, Tabzar and Ghazanfari[20a,b] examined the pore-scale investigation of a fluid capable of blocking pores and fractures deduced by return permeability and the blocking ability of a new lightweight colloidal gas aphron nanofluid (CGANF) in heterogeneous fractured/unfractured porous medium. Their results showed that CGANF micro-bubbles built up in the porous media could set up a significant snag to control filtrate loss, and model's permeability of was returned almost to its primary permeability when saturation fluid was re-injected into micro-models. Akrama and Akbarb[21] conducted a theoretical study of the fluid flow properties and heat transferred by the nanoparticle-enhanced drilling muds flowing through drilling pipes under different physical conditions. Their results revealed that the velocity profile rises for application of forwarding electric field and temperature profile greatly decays. In addition, the nanoparticle volume fraction contributes to fluid acceleration and thermal conductivity of the drilling mud.

According to the literature, no studies were performed on the parameters affecting the penetration of drilling fluid in the single fracture in the reservoir conditions with mud circulation simulation. In this research, a single metal plug fracture was used to consider only the fracture wall and eliminate the formation matrix effect for the first time to study the behavior of micro-bubble fluids, especially as drilling mud, to reduce the formation damage in the production zone. The research is formed by analyzing the influence of the important parameters, including fracture size, bubble size, and pressure differences between plug and mud circulation flow. The results of this research can be used to create more accurate designs of aphron fluid in fractured reservoir to reduce formation damage during drilling or work-over operation.

2. METHODOLOGY

2.1. Experimental Materials. To perform the experiments according to the DOE, we prepared three metal cores with different fracture widths with different mixing speeds to inspect the main parameters by our main tests. In our experimental process, we loaded each as-tested micro-bubble metal core and fluid in the experimental setup (FDS350). Then, each test was run for 30−60 min. After each test, the test equipment was adequately cleaned and prepared for the next experiment. We have repeated one of the tests with identical conditions and fluid for two new metal cores, metal core numbers 4 and 5. We explain these two additional experiments in the following.

2.2. Core Sample Specification. In this research, a metal plug was used with a long fracture from one end to the other end of the plug and parallel to the cylinder's axis. The diameter of

https://doi.org/10.1021/acsomega.2c01951
ACS Omega 2022, 7, 26246−26255

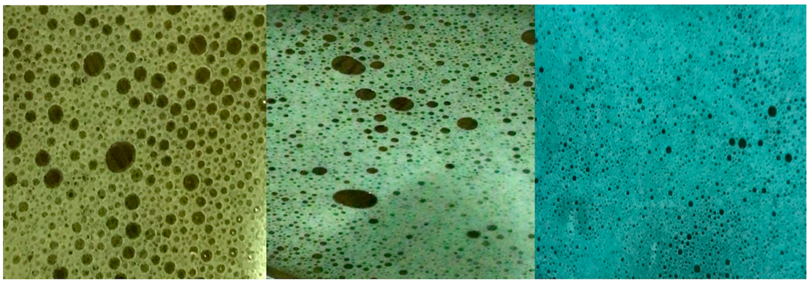

Figure 3. Micro-bubble fluid bubble size for (a) 8000, (b) 10,000, and (c) 12,000 of mixing under the microscope.

both plugs was 1.5 in., and their length was 10 cm. In order to investigate the impact of fracture width on micro-bubble fluid penetration in a single fracture and its blockage ability, three fracture widths were designed with 0.1, 0.2, and 0.25 mm sizes, which were numbered plug number 1, number 2, and number 3, respectively (Figure 1).

2.3. Properties of Fluid. In this study, a water-based fluid was used as a micro-bubble fluid. Caustic soda was added to adjust the fluid pH, and XG was employed as a stabilizer and viscosifier. The last chemical used for preparing the micro-bubble fluid was sodium dodecyl benzene sulfonate (SDBS, CMC 1.5 mM). In previous research, three micro-bubble fluids had been studied. The composition of the fluid is constant and presented in Table 1.

2.4. Experimental Procedures. *2.4.1. Micro-bubble Fluid Preparation.* To prepare micro-bubble fluid, first, caustic soda was added to water to set the pH in the range of 9.5−10. XG and SDBS were added afterward according to the concentrations in Table 1 in order to prepare the micro-bubble fluid.

A high-speed mixer was used to mix the chemicals and prepare the final micro-bubble fluid. As the mixing speed (rpm) impacts the bubble size in the final fluid, it was nominated as the second important parameter after fracture size to be studied. The three mixing speed values of 8000, 10,000, and 12,000 rpm were selected for the experiments (Figures 2 and 3).

2.4.2. Experiment Setup. Formation damage and well treatment evaluation system (FDS350) (a schematic of the system is given in Figure 4) was used to evaluate the pressure rise in the middle of plug fracture. There were four pressure gauges along the core holder, two of them in the middle of the sleeve and two others at each end of the core holder. Therefore, recording the pressure differences between these gauges during the flow showed whether the bubble blocked the fracture path in a plug or not. It also determined the blockage location in the fracture. First, the selected plug was loaded in the core holder in the sleeve because the fracture and pressure sensors faced each other. At the end of this step, overburden pressure was applied to the core sleeve.

Figure 4. Formation damage and well treatment evaluation system (FDS350) apparatus.

The next step was filling the mud transfer vessel with micro-bubble fluid and all the line paths from the mud pump to the core holder and the circulation path. The pressure difference was applied to the system software, which was related to the difference between mud circulation pressure at the front end of the plug or core holder and the flow pressure through the fracture of the plug. These pressures represented mud circulation pressure in the well-bottom and the flow pressure from a reservoir to the well, respectively, and were applied in three values of 200, 500, and 800 psi. Afterward, the test was started, and the data was recorded to be analyzed.

2.5. Design of Experiment. Since there are three essential parameters, including fracture size, mixing speed, and pressure differences in the three levels, listed in Table 2, normal study and analyses of the effect of these parameters with these levels require 27 tests. To decrease the number of tests, the Taguchi approach was employed in this research as one of the most popular procedures for designing experiments. This procedure reduced the experimental variations to gain the validated results and trends.

Table 2. Features of Experimental Design

test number	fracture size (mm)	δP (psi)	mixing speed (rpm)
1	0.1	1	8000
2	0.1	2	10,000
3	0.1	3	12,000
4	0.2	1	12,000
5	0.2	2	8000
6	0.2	3	10,000
7	0.25	1	10,000
8	0.25	2	12,000
9	0.25	3	8000

Taguchi developed a method for experimental design by which one can probe the effect of different parameters on the mean and variance of a process performance characteristic. Reducing the need to test all possible combinations, the Taguchi approach tests pairs of combinations, which saves time and resources by identifying the most influential factors in the process with the least number of experiments. His method employs orthogonal arrays based on the total number of parameters and the levels of variation for each one. The Taguchi

https://doi.org/10.1021/acsomega.2c01951
ACS Omega 2022, 7, 26246−26255

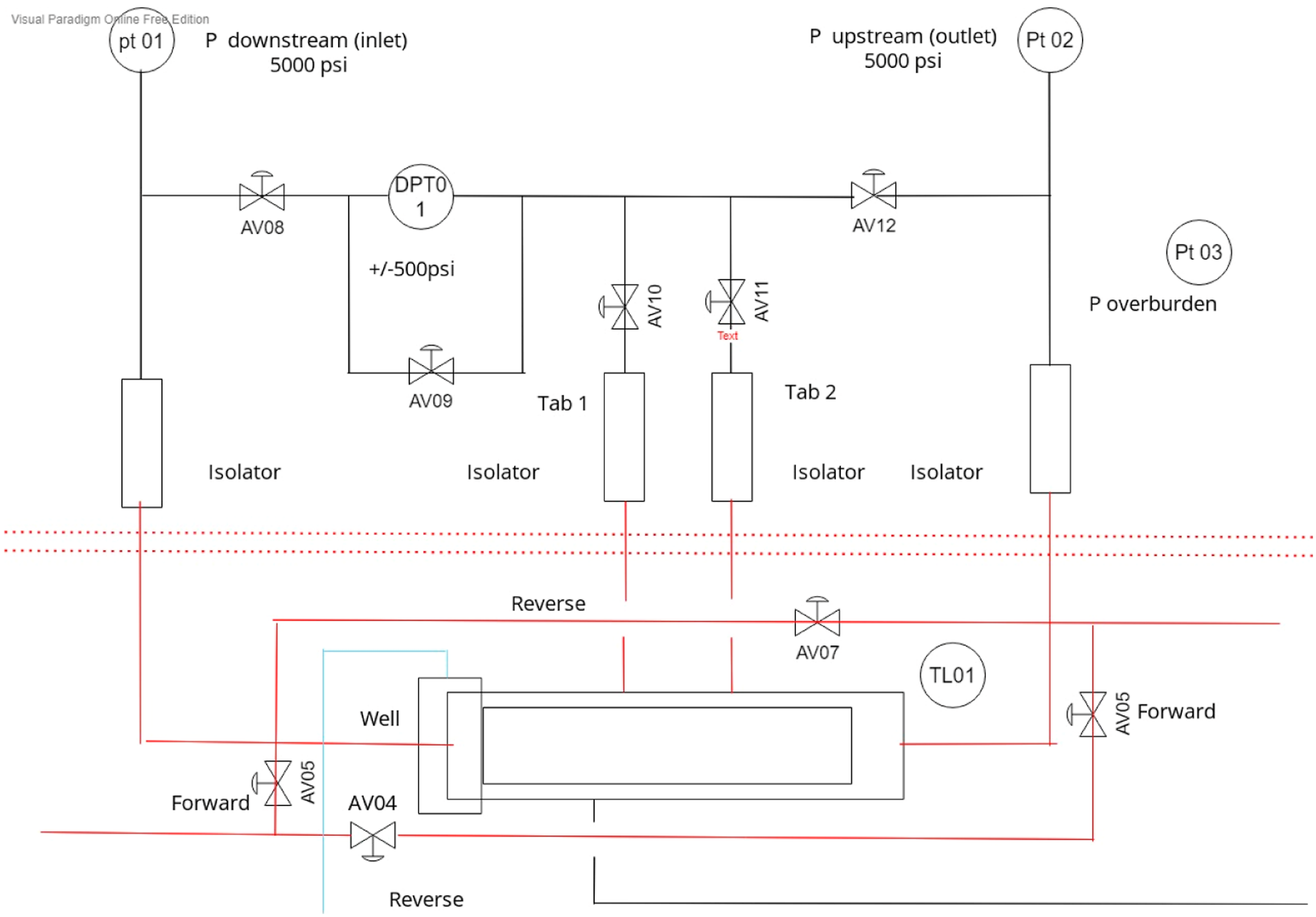

Figure 5. Piping and instrument diagram of the core holder section of FDS350 apparatus, showing the locations of pressure gauges.

method performs best when the number of variables is intermediate (3−50).

3. RESULTS AND DISCUSSION

The experiments were conducted as Table 2 features for each test. First, test numbers 1, 2, and 3 with plug number 1 were accomplished with different mixing speed and pressure difference conditions. Pressure differences between the inlet pressure transmitter (PT) and Tab1, Tab2, and outlet PT were recorded as DPT, which is illustrated in Figure 1. The system recorded the DPT every 5 s continuously. However, we had to change the desired DPT position manually to gain enough favorable data for analyzing the trends of all the three DPT and looking for a sudden rise in them. Such rises reveal blockage in that position due to bubble accumulation.

After finishing the tests, the results were exported in the graphs illustrated in Figures 7−15. In order to investigate the probable blockage locations, the setup allows us to monitor the pressure difference in three process paths. The first path starts from the inlet (well) of the core holder to valve automatic valve 10, the second path is from the inlet to valve automatic valve 11, and the third path is from the inlet to the outlet; the pressure difference between the two ends of these paths are indicated by inlet/P1, inlet/P2, and inlet/outlet, respectively (Figures 5 and 6).

A noticeable rise in the pressure difference of inlet/P2 indicates an increase in the pressure difference between the inlet and P2 (as shown in Figures 5 and 6). This increment is due to the blockage in the middle of the plug between P1 and P2.

In test number two, since the bubbles were smaller, the blockage happened later between P2 and outlet pressure gauges; this phenomenon can also be seen in the sudden rise of the pressure difference of the inlet/outlet path line in Figure 8.

Although the fracture size was similar for the first three tests, the bubble size decreased because of higher mixing speed and higher pressure on bubbles. Therefore, there was no rise in pressure differences in Figure 9, and no blockage through the fracture was observed.

In the fourth test, the fracture size was increased, as illustrated in Figure 10; the maximum mixing speed and the minimum pressure on bubbles made a bridge in the middle of the plugs between P1 and P2.

In test number 5, the pressure on the bubbles was increased while the mixing speed decreased compared to test number 4. Figure 11 shows a blockage between P1 and P2, which means the mixing speed and the bubble size are inversely related. Hence, the same bubble and fracture size cause similar blockage locations in the fracture (Figure 16).

In test number 6, the bubbles could not make a bridge through the fracture of the cores, and the pressure differences did not rise in Figure 12. This result is due to the great pressure on the bubbles and a high mixing speed.

The test results for core number 3 showed that the bubble size is sufficient to make a bridge at the last part of the fracture due to

https://doi.org/10.1021/acsomega.2c01951
ACS Omega 2022, 7, 26246−26255

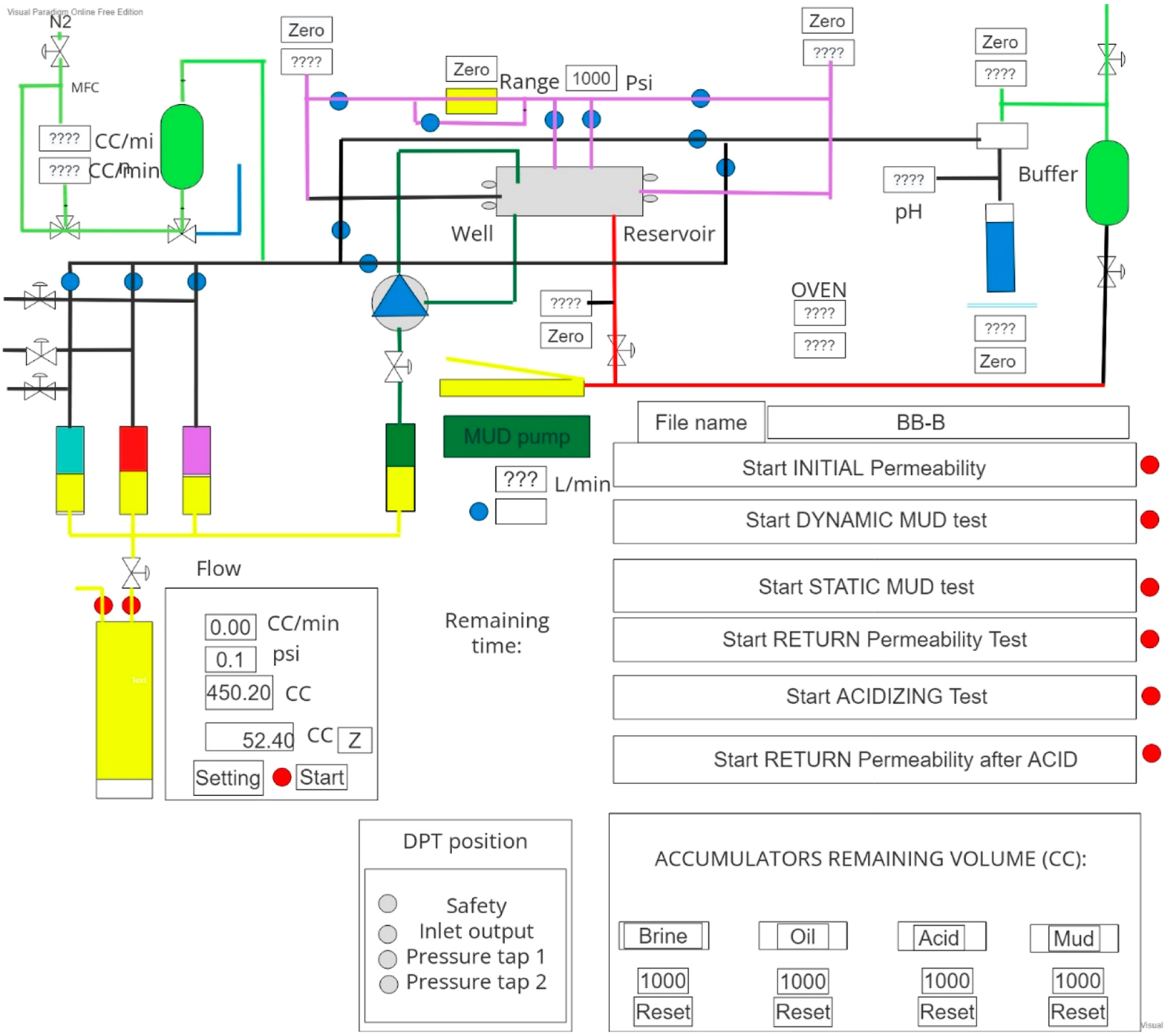

Figure 6. Schematic of formation damage and well treatment services (FDS 350).

the low pressure on the bubbles and a moderate mixing speed (Figure 13).

The decreased bubble size in test number 8 indicates no noticeable sign of a blockage in the fracture with 0.25 mm width (Figure 14).

The final test result illustrated in Figure 15 displays a sudden pressure rise because bubbles have been big enough to cause blockage at the last part of the fracture.

In comparison with previous studies which were mostly done by micro models to study the mechanism in atmospheric conditions, the experiments of this research were done under reservoir conditions for pressure and temperature. The usage of metal cores helps us to neglect the impact of fracture networks and matrix porosity, permeability, and so forth.

As we use the stable and approved the composition of the micro-bubble fluid, the focus of researchers concentrates on the desired parameters and infiltration phenomenon through the single fracture, so there is no need for searching and finding a new stable composition for the test fluid (Figure 17).

During the research, it was clear that the bubble size was reduced with a higher mixing speed. As the most important consequence, higher pressure differences and higher mixing speeds make bubbles smaller. As anticipated, smaller bubbles decrease the chance of blockage in the fractures. The blockage is important because it reduces the drilling fluid invasion in the reservoir formation. It can be produced again by the first backwash or backflow from the reservoir through the well; thus, the formation damage and well skins will decrease.

The result of this analysis is as follows. First, increasing the mixing speed delays the bubble bridging in the fracture due to the decreasing bubble size regardless of the fracture width.

Second, there is a direct relationship between the fracture size and the penetration of micro-bubble fluid into a single fracture. As the comparison between tests in the table depicts, the increase in fracture size results in deeper penetration of the fluid.

Comparing the results and diagrams of test numbers 2 and 7 in Table 3 proves the previous conclusion. The same mixing speed (Table 3) was applied in these tests. However, the 300 psi

https://doi.org/10.1021/acsomega.2c01951
ACS Omega 2022, 7, 26246−26255

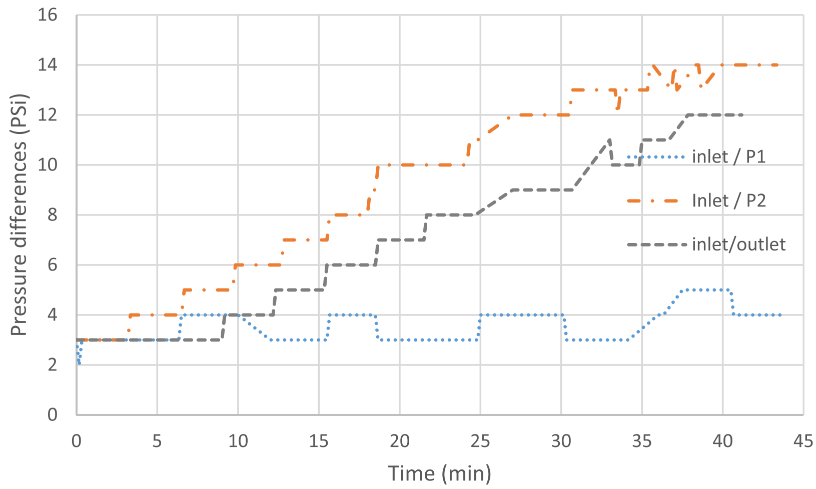

Figure 7. Pressure vs time results of test number 1 (the inlet/outlet line indicates the pressure difference between the two ends of plug in the core holder. The inlet/P1 line refers to the pressure difference between the inlet end and Tab1 through the core holder. The inlet/P2 line shows the pressure difference of inlet end and Tab2 gauge in the middle of the plug in the core holder).

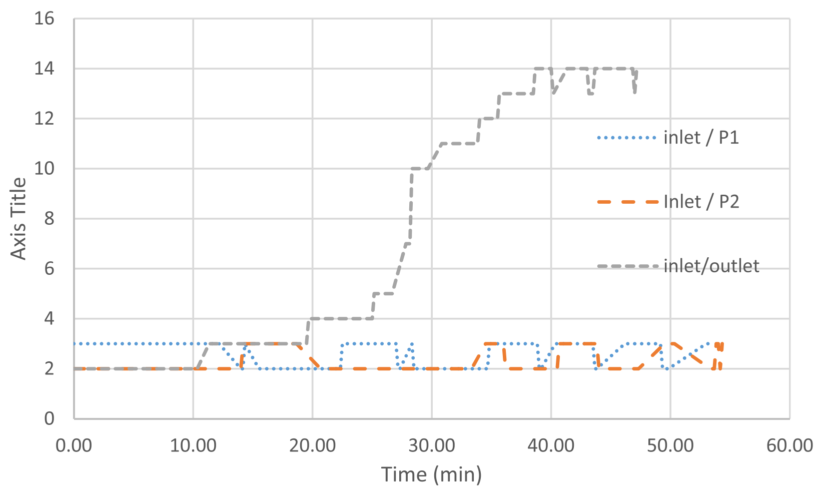

Figure 8. Pressure vs time results of test number 2 (the inlet/outlet line indicates the pressure difference between the two ends of the plug in the core holder. The inlet/P1 line refers to the pressure difference between the inlet end and Tab1 through the core holder. The inlet/P2 line shows the pressure difference of the inlet end and Tab2 gauge in the middle of the plug in the core holder).

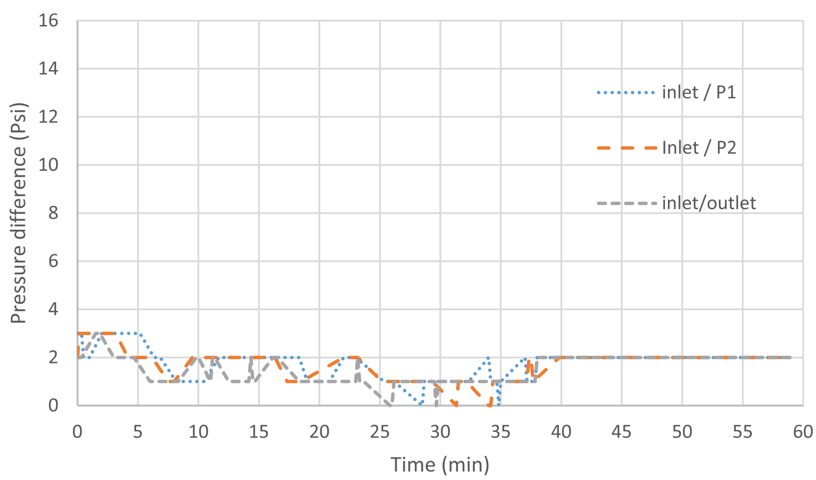

Figure 9. Pressure vs time results of test number 3 (the inlet/outlet line indicates the pressure difference between the two ends of the plug in the core holder. The inlet/P1 line refers to the pressure difference between the inlet end and Tab1 through the core holder. The inlet/P2 line shows the pressure difference of the inlet end and Tab2 gauge in the middle of the plug in the core holder).

https://doi.org/10.1021/acsomega.2c01951
ACS Omega 2022, 7, 26246−26255

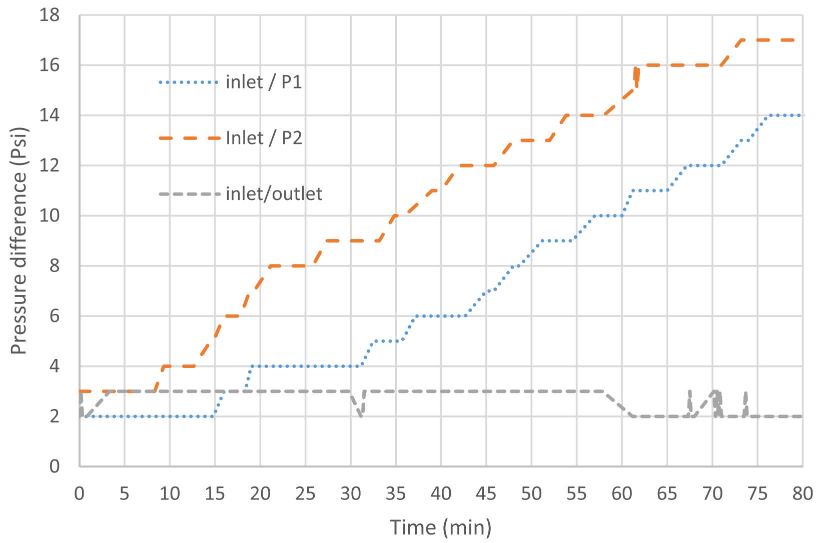

Figure 10. Pressure vs time results of test number 4 (the inlet/outlet line indicates the pressure difference between the two ends of the plug in the core holder. The inlet/P1 line refers to the pressure difference between the inlet end and Tab1 through the core holder. The inlet/P2 line shows the pressure difference of the inlet end and Tab2 gauge in the middle of the plug in the core holder).

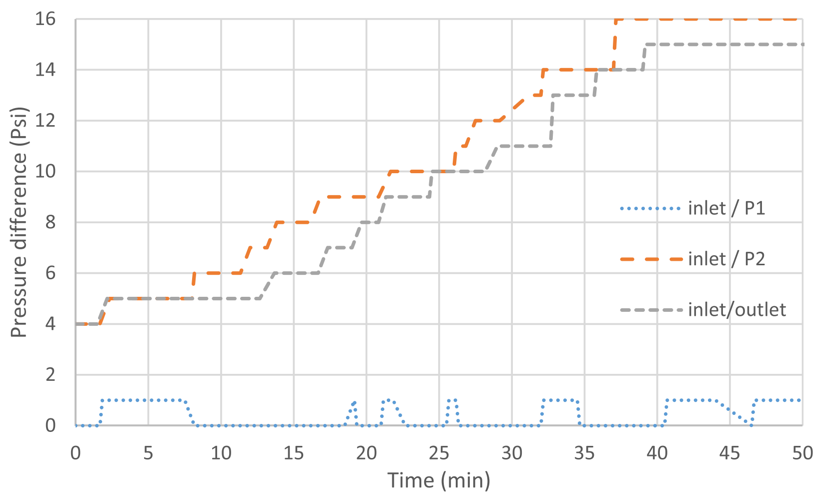

Figure 11. Pressure vs time results of test number 5 (the inlet/outlet line indicates the pressure difference between the two ends of the plug in the core holder. The inlet/P1 line refers to the pressure difference between the inlet end and Tab1 through the core holder. The inlet/P2 line shows the pressure difference of the inlet end and Tab2 gauge in the middle of the plug in the core holder).

higher pressure on the fluid bubbles in the test resulted in smaller bubbles, decreased the chance of blockage through the fracture path, and increased fluid penetration in fractured formations. Despite the fracture size in test number 7 being 2.5 times bigger than test number 2, the blockage happened in the same place at the end part of the fracture path in the core for both tests (this observation shows the importance of fracture size and can change the fluid flow behavior and other parameter influences).

Table 4 compares the micro-bubble fluid blockage ability in a porous media in previous research and this ability for a single fracture in this study. This comparison illustrates the novel achievement of this research in the field of micro-bubble fluid flow in reservoirs.

To compare the results of tests number 6 and 9, the pressure on bubbles is equal, and the fracture size is similar. However, the fluid mixing speed impacts the bubble size and significantly changes the behavior and effective fracture blocking ability. In this case, mixing speeds make bubbles smaller for test number 6 compared to test 9. At the same time, other parameters are nearly constant, so it is observed that bigger bubbles can block the fracture in the last part in test 9, but the blockage did not happen in test number 6 (Table 5).

4. CONCLUSIONS

This paper was an experimental study investigating the penetration of a micro-bubble fluid in a single fracture using a synthetic metal plug. Bubble size, fracture size, and pressure differences between the well and the reservoir were selected as important parameters to be investigated in this study. Taguchi method was utilized for the DOEs in order to minimize the number of tests, which resulted in nine tests. The outcomes are listed as follows:

- The larger bubble size or the smaller fracture size increases the chance of the creation of a bridge of bubbles more than two times, which causes blockage in a single fracture and leads to a pressure difference between two sides of the fracture.

https://doi.org/10.1021/acsomega.2c01951
ACS Omega 2022, 7, 26246−26255

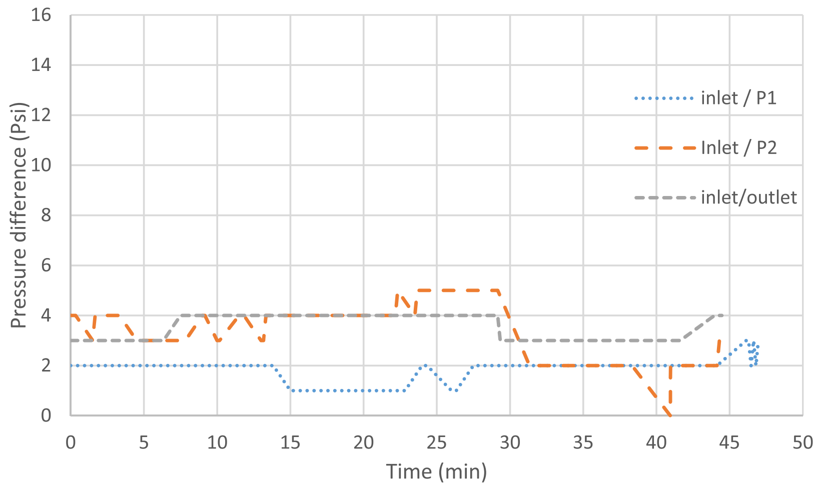

Figure 12. Pressure vs time results of test number 6 (the inlet/outlet line indicates the pressure difference between the two ends of the plug in the core holder. The inlet/P1 line refers to the pressure difference between the inlet end and Tab1 through the core holder. The inlet/P2 line shows the pressure difference of the inlet end and Tab2 gauge in the middle of the plug in the core holder).

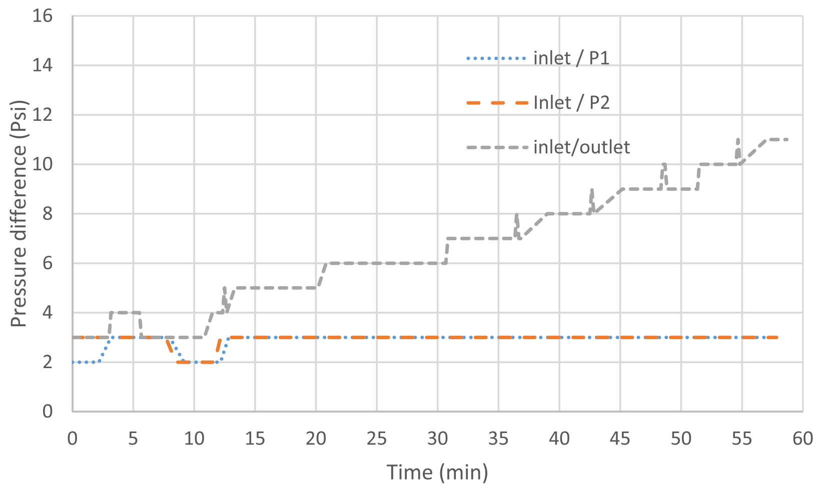

Figure 13. Pressure vs time results of test number 7 (the inlet/outlet line indicates the pressure difference between the two ends of the plug in the core holder. The inlet/P1 line refers to the pressure difference between the inlet end and Tab1 through the core holder. The inlet/P2 line shows the pressure difference of the inlet end and Tab2 gauge in the middle of the plug in the core holder).

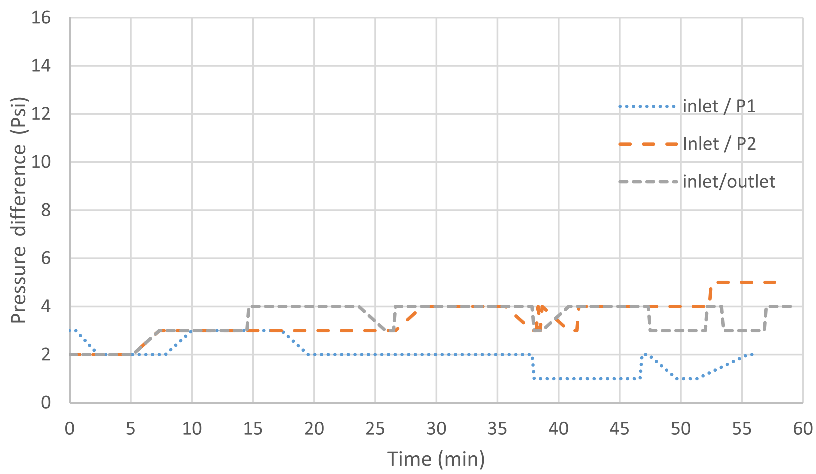

Figure 14. Pressure vs time results of test number 8 (the inlet/outlet line indicates the pressure difference between the two ends of the plug in the core holder. The inlet/P1 line refers to the pressure difference between the inlet end and Tab1 through the core holder. The inlet/P2 line shows the pressure difference of the inlet end and Tab2 gauge in the middle of the plug in the core holder).

https://doi.org/10.1021/acsomega.2c01951
ACS Omega 2022, 7, 26246−26255

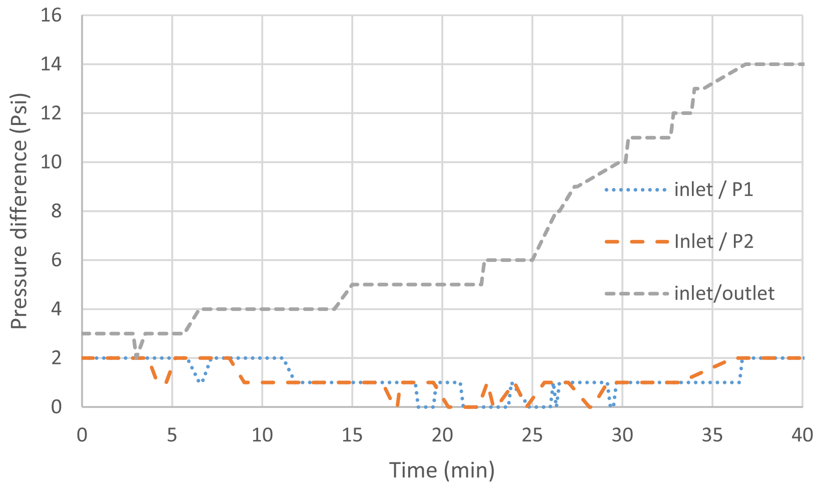

Figure 15. Pressure vs time test number 9 (the inlet/outlet line indicates the pressure difference between the two ends of the plug in the core holder. The inlet/P1 line refers to the pressure difference between the inlet end and Tab1 through the core holder. The inlet/P2 line shows the pressure difference of the inlet end and Tab2 gauge in the middle of the plug in the core holder.

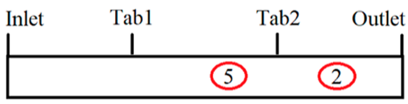

Figure 16. Schematic of blockage locations in the fracture for test numbers 2, 5, and 8.

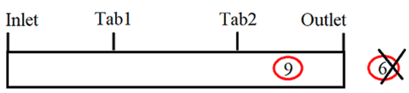

Figure 17. Schematic of blockage locations in the fracture for tests 6 and 9.

Table 3. Test Number 2 and 7 Comparison and Analysis

test number	fracture size (mm)	δP (psi)	mixing speed (rpm)	bubble size	blockage location
2	0.1	2	10,000	small	third part
7	0.25	1	10,000	big	third part

- Bubble size is several times more important than fracture size. As shown, the minimum size of the bubble in the minor fracture size cannot cause the bubble blockage, but the medium size of the bubble in the large size of fracture blocks the fracture path.
- In the reservoir zones, the employment of a micro-bubble drilling fluid with the minimum over the balance drilling condition (near 200 psi) not only decreases the flow loss in drilling operation but also impressively increases the bubble bridge formation in fractured zones with any mixing speed or fracture size (formation damage reduction and bubble blockage will happen absolutely).
- Controlling the size of bubbles using low mixing rpm and low-pressure flow leads to less drilling fluid penetration in the fracture and minor formation damage; however, when operators set it in the range of 8000 rpm, they can expect to have bubble bridging in different sizes of fracture up to 0.25 mm and in an overbalanced drilling range of 200–800 psi.
- Fracture walls' roughness is entirely effective for trapping the bubbles on the surface for fracture. The roughness helps bubbles accumulate and make bridges to reduce the formation damage and mud or fluid infiltration.

Table 5. Test Number 6 and 9 Comparison and Analysis

test number	fracture size (mm)	δP (psi)	mixing speed (rpm)	bubble size	blockage location
6	0.2	3	10,000	small	no blockage
9	0.25	3	8000	big	third part

■ AUTHOR INFORMATION

Corresponding Author

Ehsan Khamehchi – *Department of petroleum engineering, Amirkabir University of Technology, Tehran 1591634311, Iran*; orcid.org/0000-0002-3907-6104; Email: khamehchi@aut.ac.ir

Authors

Sina Baseli Zadeh – *Department of petroleum engineering, Amirkabir University of Technology, Tehran 1591634311, Iran*; orcid.org/0000-0003-4706-5760

Saeed Saber-Samandari – *New Technologies Research Center, Amirkabir University of Technology, Tehran 1591634311, Iran*

Ali Alizadeh – *Department of petroleum engineering, Amirkabir University of Technology, Tehran 1591634311, Iran*

Complete contact information is available at:

Table 4. Comparison of Micro-bubble Fluid Blockage Ability in a Porous Media and a Single Fracture from Previous Research and the Present Study

paper name/year	conclusion for porous media from the previous paper	the conclusion from this study for the single fracture
a study of the pore-blocking ability and formation damage characteristics of oil-based colloidal gas aphron drilling fluids/(2014)	the effective pore-blocking ability of micro-bubble fluid was confirmed by a continuous increase of pressure drop across the porous media while the micro-bubble fluid was injected at a constant rate	effective fracture blocking ability of micro-bubble fluid was confirmed by the continuous increase of pressure drop across the fracture while the micro-bubble fluid was injected at a constant rate

https://doi.org/10.1021/acsomega.2c01951
ACS Omega 2022, 7, 26246−26255

https://pubs.acs.org/10.1021/acsomega.2c01951

Notes

The authors declare no competing financial interest.

REFERENCES

(1) (a) Belkin, A.; Irving, M.; O'Connor, B.; Fosdick, M.; Hoff, T. L.; Growcock, F. B. *How Aphron Drilling Fluids Work*, SPE Annual Technical Conference and Exhibition; OnePetro, 2005. (b) Feng, W.; Singhal, N.; Swift, S. Drainage mechanism of microbubble dispersion and factors influencing its stability. *J. Colloid Interface Sci.* **2009**, *337*, 548−554. (c) Brookey, T.; Rea, A.; Roe, T. *UBD and Beyond: Aphron Drilling Fluids for Depleted Zones*, IADC World Drilling Conference: Vienna, Austria, 2003. (d) Mohammadi, M. K.; Riahi, S.; Boek, E. S. An insight review on formation damage induced by drilling fluids. *Rev. Chem. Eng.* **2022**, DOI: 10.1515/revce-2020-0106.

(2) He, X. *The Past, Present and Future of Aphron Based Drilling Fluids*, SPE Annual Technical Conference and Exhibition; OnePetro, 2010.

(3) (a) Growcock, F. B.; Simon, G. A.; Rea, A. B.; Leonard, R. S.; Noello, E.; Castellan, R. *Alternative Aphron-Based Drilling Fluid*, IADC/SPE Drilling Conference; OnePetro, 2004. (b) Mirabbasi, S. M.; Ameri, M. J.; Alsaba, M.; Karami, M.; Zargarbashi, A. The evolution of lost circulation prevention and mitigation based on wellbore strengthening theory: A review on experimental issues. *J. Petrol. Sci. Eng.* **2022**, *211*, 110149.

(4) Ivan, C.; Quintana, J.; Blake, L. *Aphron-Base Drilling Fluid: Evolving Technologies for Lost Circulation Control*, SPE Annual Technical Conference and Exhibition; OnePetro, 2001.

(5) Montilva, J.; Ivan, C. D.; Friedheim, J.; Bayter, R. *Aphron Drilling Fluid: Field Lessons from Successful Application in Drilling Depleted Reservoirs in Lake Maracaibo*; Offshore Technology Conference; OnePetro, 2002.

(6) Roy, D.; Valsaraj, K. T.; Kottai, S. A. Separation of organic dyes from wastewater by using colloidal gas aphrons. *Sep. Sci. Technol.* **1992**, *27*, 573−588.

(7) (a) Sebba, F. *Foams and Biliquid Foams, Aphrons*; Wiley, 1987. (b) White, C. C.; Chesters, A. P.; Ivan, C. D.; Maikranz, S.; Nouris, R. Aphron-based drilling fluid: Novel technology for drilling depleted formations: Drilling report. *World Oil* **2003**, *224*, 37−43.

(8) Ramirez, F.; Greaves, R.; Montilva, J. *Experience Using Micro-bubbles-Aphron Drilling Fluid in Mature Reservoirs of Lake Maracaibo*, International Symposium and Exhibition on Formation Damage Control; OnePetro, 2002.

(9) Bjorndalen, N.; Kuru, E. *Stability of Microbubble Based Drilling Fluids under Downhole Conditions*, Canadian International Petroleum Conference; OnePetro, 2006.

(10) Spinelli, L. S.; Neto, G. R.; Freire, L. F. A.; Monteiro, V.; Lomba, R.; Michel, R.; Lucas, E. Synthetic-based aphrons: correlation between properties and filtrate reduction performance. *Colloids Surf., A* **2010**, *353*, 57−63.

(11) (a) Nareh'ei, M. A.; Shahri, M. P.; Zamani, M. Rheological and filtration loss characteristics of colloidal gas aphron based drilling fluids. *J. Jpn. Pet. Inst.* **2012**, *55*, 182−190. (b) Arabloo, M.; Pordel Shahri, M. Experimental studies on stability and viscoplastic modeling of colloidal gas aphron (CGA) based drilling fluids. *J. Petrol. Sci. Eng.* **2014**, *113*, 8−22. (c) Bjorndalen, H. N.; Jossy, W. E.; Alvarez, J. M.; Kuru, E. A laboratory investigation of the factors controlling the filtration loss when drilling with colloidal gas aphron (CGA) fluids. *J. Petrol. Sci. Eng.* **2014**, *117*, 1−7. (d) Shivhare, S.; Kuru, E. A study of the pore-blocking ability and formation damage characteristics of oil-based colloidal gas aphron drilling fluids. *J. Petrol. Sci. Eng.* **2014**, *122*, 257−265. (e) Ziaee, H.; Arabloo, M.; Ghazanfari, M. H.; Rashtchian, D. Herschel−Bulkley rheological parameters of lightweight colloidal gas aphron (CGA) based fluids. *Chem. Eng. Res. Des.* **2015**, *93*, 21−29.

(12) Zheng, L.-h.; Wang, J.-f.; Li, X.-p.; Zhang, Y.; Li, D. Optimization of rheological parameter for micro-bubble drilling fluids by multiple regression experimental design. *J. Cent. South Univ. Technol.* **2008**, *15*, 424−428.

(13) Alizadeh, A.; Khamehchi, E. Modeling of micro-bubble surfactant multi-layer drilling fluid stability based on single bubble behavior under pressure and temperature in a deviated gas well. *J. Nat. Gas Sci. Eng.* **2015**, *26*, 42−50.

(14) (a) Alizadeh, A.; Khamehchi, E. Mathematical modeling of the colloidal gas aphron motion through porous medium, including colloidal bubble generation and destruction. *Colloid Polym. Sci.* **2016**, *294*, 1075−1085. (b) Alizadeh, A.; Khamehchi, E. Stability modeling of water-based surfactant covered micro-bubble fluids. *J. Surfactants Deterg.* **2016**, *19*, 165−171.

(15) Alizadeh, A.; Khamehchi, E. A model for predicting size distribution and liquid drainage from micro-bubble surfactant multi-layer fluids using population balance. *Colloid Polym. Sci.* **2015**, *293*, 3419−3427.

(16) Keshavarzi, B.; Javadi, A.; Bahramian, A.; Miller, R. Formation and stability of colloidal gas aphron based drilling fluid considering dynamic surface properties. *J. Petrol. Sci. Eng.* **2019**, *174*, 468−475.

(17) Zhu, W.; Zheng, X.; Li, G. Micro-bubbles size, rheological and filtration characteristics of Colloidal Gas Aphron (CGA) drilling fluids for high temperature well: Role of attapulgite. *J. Petrol. Sci. Eng.* **2020**, *186*, 106683.

(18) Le, N. N. H.; Sugai, Y.; Sasaki, K. Investigation of Stability of CO2 Microbubbles—Colloidal Gas Aphrons for Enhanced Oil Recovery Using Definitive Screening Design. *Colloids Interfaces* **2020**, *4*, 26.

(19) Zhu, W.; Zheng, X.; Shi, J.; Wang, Y. A high-temperature resistant colloid gas aphron drilling fluid system prepared by using a novel graft copolymer xanthan gum-AA/AM/AMPS. *J. Petrol. Sci. Eng.* **2021**, *205*, 108821.

(20) (a) Tabzar, A.; Ghazanfari, M. H. Monitoring of microscopic behavior of nano-enhanced colloidal gas aphron in fractured and un-fractured non-uniform porous medium. *J. Petrol. Sci. Eng.* **2021**, *210*, 110073. (b) Tabzar, A.; Ghazanfari, M. H. Monitoring of microscopic behavior of nano-enhanced colloidal gas aphron in fractured and un-fractured non-uniform porous medium. *J. Petrol. Sci. Eng.* **2022**, *210*, 110073.

(21) Akrama, J.; Akbarb, N. S. Mathematical Modeling of Aphron Drilling nanofluid Driven by Electroosmotically Modulated Peristalsis Through a Pipe. *Math. Model Nat. Phenom.* **2017**, DOI: 10.1051/mmnp/2022012.